

Catalysis Science & Technology

Accepted Manuscript



This is an *Accepted Manuscript*, which has been through the Royal Society of Chemistry peer review process and has been accepted for publication.

Accepted Manuscripts are published online shortly after acceptance, before technical editing, formatting and proof reading. Using this free service, authors can make their results available to the community, in citable form, before we publish the edited article. We will replace this *Accepted Manuscript* with the edited and formatted *Advance Article* as soon as it is available.

You can find more information about *Accepted Manuscripts* in the [Information for Authors](#).

Please note that technical editing may introduce minor changes to the text and/or graphics, which may alter content. The journal's standard [Terms & Conditions](#) and the [Ethical guidelines](#) still apply. In no event shall the Royal Society of Chemistry be held responsible for any errors or omissions in this *Accepted Manuscript* or any consequences arising from the use of any information it contains.



Catalysis Science & Technology

ARTICLE

Structure-controlled Porous Films of Nanoparticulate Rh-doped SrTiO₃ Photocatalyst toward Efficient H₂ Evolution under Visible-light Irradiation

Received 00th January 2015,
Accepted 00th January 2015

DOI: 10.1039/x0xx00000x

www.rsc.org/

Sayuri Okunaka^{a,b}, Hiromasa Tokudome^{a*} and Ryu Abe^{b*}

Porous films of Rh-doped SrTiO₃ (SrTiO₃:Rh) were prepared on glass substrates as a visible-light responsive photocatalyst panel that can generate H₂ efficiently under visible light irradiation. The films were prepared by simple screen-printing using pastes of fine particles (ca. 50 nm) of SrTiO₃:Rh (WH-particles), which were prepared *via* a facile water-based process, followed by calcination at 500°C. The use of WH-particles having relatively narrow size distribution allowed us to prepare homogeneous films with controlled thickness ranging from 1 to 10 μm, along with enough mechanical strength. On the other hand, the use of SrTiO₃:Rh particles (SS-particles, ca. 300 nm) prepared by conventional solid state reaction method resulted in inhomogeneous surfaces and exposure of the glass substrates when the thickness was below 3 μm. The SrTiO₃:Rh films (WH-films) consisting of the fine particles exhibited much higher efficiency for H₂ evolution from methanol aqueous solution under visible light than those prepared from the SS-particles (SS-films) at each thickness. The H₂ evolution rate on WH-films increased to reach maximum value at 10 μm (3.2 μmol/h) while those on SS-films saturated at a thinner thickness of 5 μm (0.7 μmol/h), and was confirmed to be higher than those on the suspended system with the same amounts of WH-particles. Furthermore, the addition (10–20 wt%) of the large particles to the WH-films further increased the H₂ evolution rate probably due to the light scattering with large SS-particles, by which the neighboring small WH-particles in the films can effectively absorb the scattered light and generate more H₂.

Introduction

Photocatalytic water splitting using semiconductors has attracted much attentions as technology that can produce hydrogen (H₂) directly from water by harvesting abundant solar light.¹ The design of photocatalytic systems that enable efficient utilization of wide range of solar light spectrum, especially in visible region has become one of the cutting-edge research areas for achieving practically sufficient efficiency in solar hydrogen production, as well as the development of semiconductor materials employed.^{2–4} So far, two types of semiconductor-based systems have extensively been studied for photo-induced water splitting; one is heterogeneous system^{5–8} with suspended semiconductor particles and the other is photoelectrochemical system^{8–10} with semiconductor photoelectrodes. The former suspended system has, however, some disadvantages in large-scale applications.¹¹ Such heterogeneous system undoubtedly require the energy for keeping the semiconductor particles suspended in the solution,

by mean of mechanical stirring or gas-bubbling, and also required separation of particles for the recycling or replacing the used photocatalysts. Although these problems can be solved in the later photoelectrochemical systems, in which semiconductor materials are generally fixed on substrates, other cost disadvantages come up to the surface, i.e., the costs for the conductive substrates (such as conductive glass or metals) and for the external circuit including power source. Photocatalyst panels, wherein semiconductor particles are fixed on a inexpensive substrate such as glass, will be another candidate of cost-effective and efficient water splitting system, if they exhibit comparable (or higher) efficiency to those in conventional systems.^{11,12} Recently, Domen et al. demonstrated simultaneous evolution of H₂ and O₂ under UV-vis irradiation using photocatalyst panels of GaN-ZnO solid solution semiconductor prepared *via* drop-casting or squeegee method.¹¹ However, there is only a few report on the water splitting using such kinds of photocatalyst panels.^{11–13} Thus detailed and systematic studies on photocatalyst panels are highly desired to evaluate their feasibility by examining the influences of various factors such as types of semiconductor and structure of films on the performance. It is expected that high performance photocatalyst panels should have both the controlled structures for efficient light absorption and the controlled pores allowing efficient reaction and transportation of substances. However, such well-designed panels are generally difficult to be fabricated by using the semiconductor particles prepared *via*

^a Research Institute, TOTO LTD., 2-8-1 Hanson, Chigasaki-City, Kanagawa-pref. 253-8577, Japan. Fax: +81 467 54 1185; Tel: +81 467 54 3483; E-mail: hiromasa.tokudome@jp.toto.com

^b Department of Energy and Hydrocarbon Chemistry, Graduate School of Engineering, Kyoto University, Katsura Nishikyo-ku, Kyoto 615-8510, Japan. Fax: +81-75-383-2478; Tel: +81-75-383-2478; E-mail: ryu-abe@scl.kyoto-u.ac.jp
Electronic Supplementary Information (ESI) available: UV-vis spectrum, SEM images, photocatalytic H₂ evolving reaction data. See DOI: 10.1039/x0xx00000x

conventional synthesis processes such as solid-state (SS) reaction, in which large and inhomogeneous particles are generally produced.¹⁴ The use of semiconductor particles having well-controlled particle sizes, specifically in nano~submicron regions, is highly desirable to fabricate such well-designed photocatalyst panels; the use of such fine particles will be also beneficial to ensure the mechanical strength of panels by forming good adhesion.¹⁵

We have recently reported a facile synthesis of fine particles of Rh doped SrTiO₃ (SrTiO₃:Rh) semiconductor, which is well known as one of the promising materials of visible light responsive photocatalyst for H₂ production¹⁶⁻²⁵, via a newly-developed water-based hetero-chelate method using a stable aqueous titania sol²⁷ as a precursor with other metal salts.²⁸ The prepared SrTiO₃:Rh particles possessed homogeneous and small particle size (ca. 50 nm) and exhibited significantly high efficiency for H₂ evolution from aqueous methanol solution under visible light irradiation (ca. 13.3% of quantum efficiency at 420 nm).²⁸ These findings have motivated us to apply the SrTiO₃:Rh fine particles as a model photocatalyst to the fabrication of photocatalyst panels that can efficiently generate H₂ under visible light. In this paper, we attempted to prepare the porous SrTiO₃:Rh films having both the controlled thickness and pores from the nanoparticulate SrTiO₃:Rh by means of simple screen-printing and applied them for photocatalytic H₂ production under visible light.

Experimental

Materials

Titanium(IV) tetraisopropoxide (TIPT) (95.0%), acetylacetone (acac) (99.0%), acetic acid (AcOH) (99.7%), strontium acetate hemihydrate (Sr(OAc)₂·0.5H₂O), rhodium(III) chloride trihydrate (RhCl₃·3H₂O), lactic acid (85.5–94.5%), Rh₂O₃, α -terpineol, 2-(2-butoxyethoxy)ethanol and poly(vinyl butyral) were purchased from Wako Pure Chemical Industries, Ltd., Osaka, Japan. Acrylic emulsion (VONCOAT (EC-905EF), particle size: 100–150 nm) was purchased from DIC Corporation. TiO₂ (99.9%) was purchased from Soekawa chemical. SrCO₃ (99.9%) was purchased from Kanto chemical. All reagents were used as received, and all the experiments were carried out under ambient condition without eliminating the moisture from the atmosphere.

Preparation of SrTiO₃:Rh films

The particles of SrTiO₃:Rh(2%) were prepared via the water-based hetero-chelate method (WH-method), which was recently developed by our group,²⁸ using a stable titania sol²⁷ as a precursor. The aqueous titania sol (AA-sol) was prepared by mixing TIPT, an aqueous solution of acac, and an aqueous solution of AcOH.²⁷ The AA-sol was mixed with an aqueous solution containing both Sr(OAc)₂ (1.08 mol/L) and lactic acid (2.16 mol/L) and an aqueous solution of RhCl₃ (0.24 mol/L) at the ratio of Sr:Ti:Rh = 1.02:0.98:0.02, and stirred for 1 hour at room temperature, yielding an orange transparent sol. The sol was added by an acrylic emulsion and stirred for 15 minutes at room temperature, then dried at 80°C for 3 hours, and finally

calcined at 1000°C for 10 hours, yielding SrTiO₃:Rh(Rh: 2%) powdered samples (these samples will be denoted by WH-particles). For comparison, SrTiO₃:Rh(2%) particles were also prepared via the solid state reaction method (SS-method) using from TiO₂, SrCO₃ and Rh₂O₃ as raw materials, and following calcination at 1000°C for 10 hours (these samples will be denoted by SS-particles). Although some reports have suggested that the addition of excess Sr in the preparation of SrTiO₃-based particles via the SS-method is effective to obtain more active photocatalyst samples, we confirmed that the SrTiO₃:Rh particles prepared via the SS-method with excess amount of Sr (Sr/(Ti+Rh) = 1.03, for example) showed almost same rate of H₂ evolution as that on the sample prepared with the stoichiometric ratio.²⁸ Thus in the present study, the SrTiO₃:Rh particles prepared via the SS-method with stoichiometric ratio (Sr:(Ti+Rh) = 1) was employed as the almost best SS-sample for fabricating SrTiO₃:Rh films for comparison. As an effective cocatalyst for water reduction, small amount (0.5 wt%) of platinum particles were loaded on all the samples by mean of in-situ photodeposition method.^{16,17,28}

The SrTiO₃:Rh(2%) films were prepared via a conventional screen printing method as follows. The WH- or SS-particles were first dispersed in methanol solution and then dried at 80°C for 5 min. After dispersion process, the particles were mixed with organic compounds (α -terpineol: 2-(2-butoxyethoxy)ethanol: poly(vinyl butyral) = 60:15:25) as vehicles, yielding the paste of WH- or SS-particles (ca. 20 wt%) having an appropriate viscosity for screen-printing. Films were then prepared by screen-printing using the prepared pastes, followed by calcination in air at 500°C for 30 min. To control the thickness, the screen-printing procedure was repeated (1–10 times) before calcination; the obtained films will be denoted as WH- or SS-x where x (x = 1–10) indicates the times of print repetition. To obtain the thicker film having same thickness as to WH-10 and SS-10 without repeating the printing process, another setup of screen-printing with a thicker screen was used. The obtained films will be named WH-10' and SS-10'.

Characterization of SrTiO₃:Rh films

The obtained SrTiO₃:Rh films were characterized by mean of a scanning electron microscope (SEM, HITACHI, S-4100), an X-ray diffraction (XRD, PANalytical, X'Pert Pro, rotating anode diffractometer, 45 kV, 40 mA, Cu K λ radiation). The photocatalytic activity of SrTiO₃:Rh(2%) films was evaluated for the H₂ evolution from aqueous methanol solution under visible light irradiation, using a gas-closed circulation system equipped with a top-irradiation type reaction cell (Pyrex-made), in which the photocatalyst film was fixed horizontally in the solution. The light irradiation was carried out from the top of reactor by a 300W Xe-arc lamp (Perkin-Elmer, Cemax PE300BF) attached with a cut-off filter (Hoya; L42) to eliminate the UV light. The amounts of gas produced were analyzed and quantified by means of an on-line gas chromatograph (GL Science; GC-3200, TCD, Ar carrier, MS-5A column).

Results and discussion

Characterizations of SrTiO₃:Rh films prepared *via* screen-printing method

Fig. 1 and 2 show the SEM images of the films that were prepared *via* screen-printing with the pastes of SrTiO₃:Rh(2%) particles followed by calcination at 500°C for 30 min. The thickness of the films was controlled by changing the repeated numbers of the screen-printing before calcination or by using another setup. The SEM images of WH-*x* films (“*x*” represent the repeated numbers) revealed that the film thickness increased by ca. 1 μm with increasing numbers of the screen-printing repetition (see Fig. 1 and Fig S1). For example, the film thickness of WH-1, 3, 5 and 10’ were about 1, 3, 5 and 10 μm, respectively. In addition, all the WH-films exhibit flat surfaces.

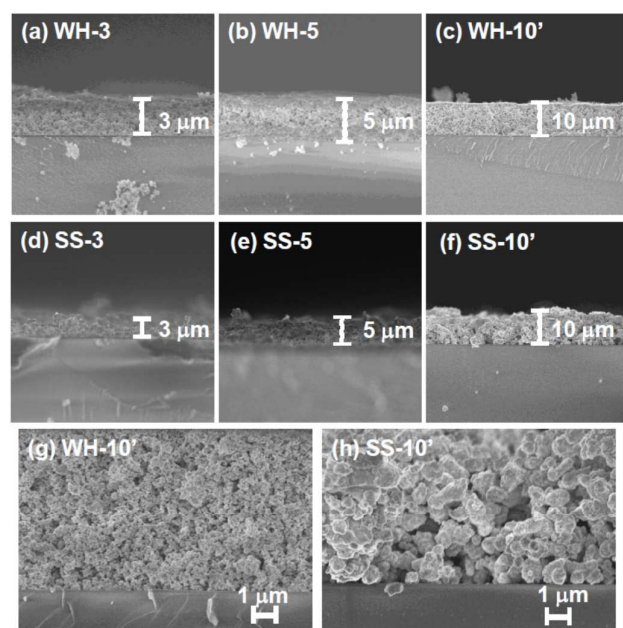


Fig. 1 Cross-sectional SEM images of SrTiO₃:Rh films (WH- and SS-films) with different thickness.

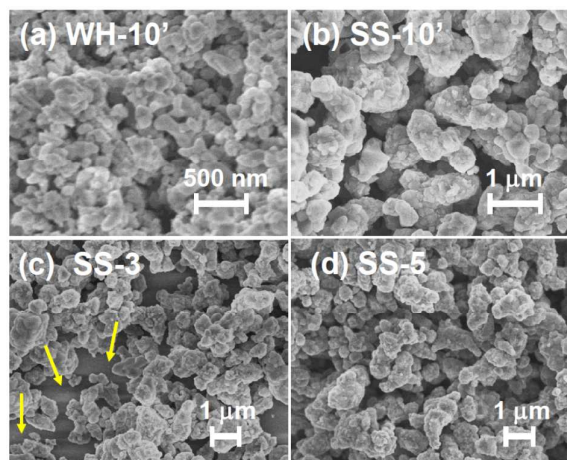
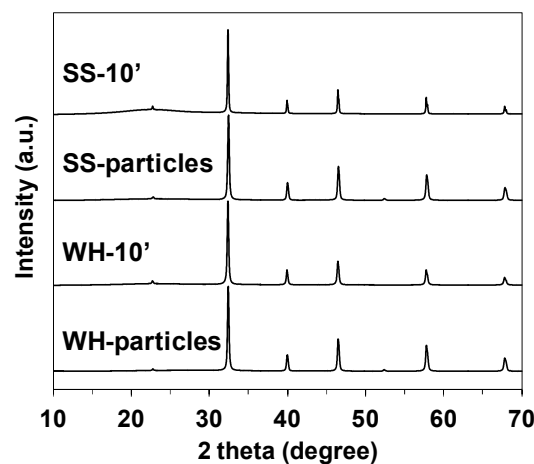


Fig. 2 Surface SEM images of SrTiO₃:Rh films (WH- and SS-films) with different thickness. Yellow arrowed lines show the uncovered parts of substrate.

It was also confirmed that the WH-10’ film, which was prepared by using a thicker screen, possessed almost same thickness (ca. 10 μm) as to that of WH-10 (see Fig. S1(e)), indicating the availability of such thicker screen for fabricating thicker films without repetition of screen printing. The flat surface morphology and uniform increment in thickness are certainly due to the homogeneously small size of WH-particles (ca. 50 nm, see Fig. S1), which were prepared *via* newly developed water-based procedure. On the other hand, the surfaces of SS-films, especially in the case of thinner ones (SS-1, SS-3), were not smooth as seen in Fig. S2(d) and Fig. 1(d), while the thickness actually increased roughly in proportion with the increasing numbers of the screen-printing. The inhomogeneous and large size of SS-particles (ca. 200–500 nm, see Fig S3) is undoubtedly one of the causes for the rough surfaces of SS-films. The magnified views of the cross-section revealed that both the WH-10’ and SS-10’ films have densely-packed porous structures (Fig. 1(g), (h)). Fig. 2 shows the top-view SEM images of WH- and SS-films (*x* = 3, 5, 10’). All the WH-films were exhibits smooth surfaces without exposing the glass substrates, even in the case of thinner one (see Fig. S2(a)-(c)). On the other hand, uncovered parts of substrate were clearly observed for thinner SS-3 sample (see Fig. 2(c)), while the repeated printing improved the homogeneity to some extent (see SS-5, 10’ in Fig. 2(b) and (d)). These findings indicated the difficulty in preparing thin films with well-controlled structures from the SS-particles.

As clearly seen in the SEM images, the WH- and SS-films were composed of the SrTiO₃:Rh particles whose primary particle sizes were almost same as those of WH- or SS-particles (see Fig. S3). The XRD patterns of WH- and SS-films showed a single phase of SrTiO₃; no appreciable peaks attributed to impurity phase was observed (Fig. 3). The diffuse reflectance spectra of WH- and SS-films (Fig. 4) were similar to those reported for SrTiO₃:Rh particles.²⁸ The two absorption bands were observed at around 420 nm and 580 nm, which are attributed to the transitions from the donor levels formed by the Rh³⁺ species to the conduction band (2.3 eV), and from the



ARTICLE

Catalysis Science & Technology

Fig. 3 XRD patterns of SrTiO₃:Rh films (WH- and SS-films) and particles (WH- and SS-particles).

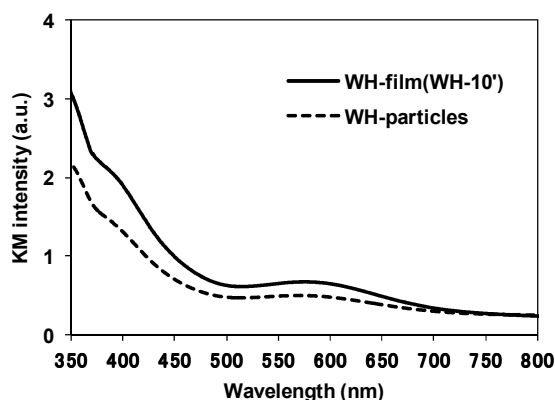


Fig. 4 UV-vis spectra of SrTiO₃:Rh films (WH-10') and SrTiO₃:Rh particles (WH-particles).

valence band to the acceptor levels formed by the Rh⁴⁺ species (1.7 eV), respectively. These results indicated that the particles contained in WH- and SS-films retained the physicochemical properties of the original WH- and SS-particles, even after the preparation process accompanied by final calcinations at 500°C. As demonstrated above, the screen printing of appropriate pastes of WH-particles, which possess uniformly small size (ca. 50 nm), was proven as an effective way for fabricating porous films of SrTiO₃:Rh with homogenous and controllable thickness ranging from 1 to 10 μ m.

Photocatalytic H₂ evolution from aqueous methanol solution under visible light on SrTiO₃:Rh films

The photocatalytic activity of these SrTiO₃:Rh(2%) films was evaluated for the H₂ evolution from aqueous methanol solution under visible light irradiation ($\lambda > 410$ nm). As an effective co-catalyst for water reduction, 0.5 wt% of platinum particles were loaded on the WH-1000 or SS-1000 samples by means of in-situ photodeposition method²⁸ prior to the preparation of paste. All the WH- and SS-films showed the photocatalytic activity for H₂ evolution from aqueous methanol solution under visible

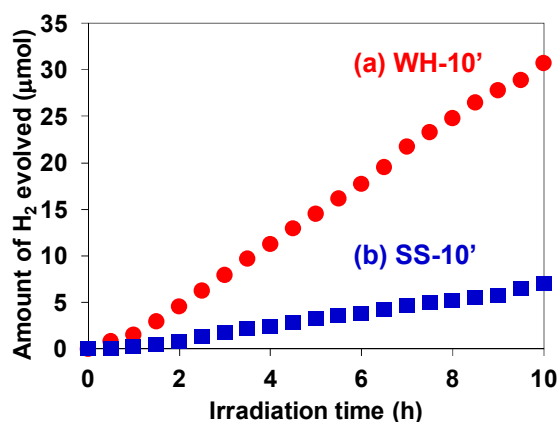


Fig. 5 H₂ evolution from an aqueous methanol solution under visible light irradiation over a SrTiO₃:Rh film ((a) WH-10' or (b) SS-10'). Conditions: 3 × 3 cm film; reactant solution, 100 mL of 10 vol% aqueous methanol solution; light source, 300 W Xe lamp with cut-off filters ($\lambda > 410$ nm).

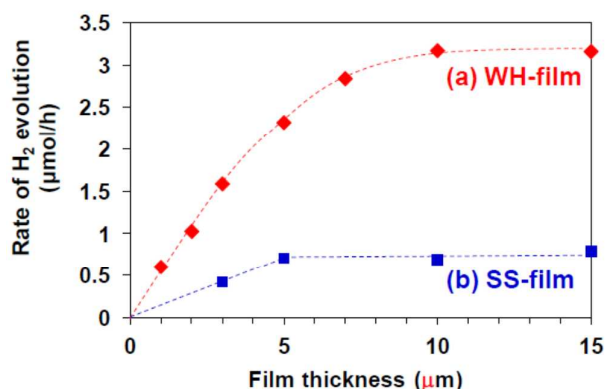


Fig. 6 Rate of H₂ evolution from an aqueous methanol solution under visible light irradiation over a SrTiO₃:Rh film having different thickness. Conditions: 3 × 3 cm film; reactant solution, 100 mL of 10 vol% aqueous methanol solution; light source, 300 W Xe lamp with cut-off filters ($\lambda > 410$ nm).

light irradiation ($\lambda > 410$ nm) with almost steady rate. The time courses of H₂ evolution on WH-10' and SS-10' are shown in Fig. 5, for example, in which the H₂ evolution rate on WH-film was about 4 times higher than that on SS-film. During the reaction, the color of WH-film changed from gray to pale yellow (see Fig. S5), indicating the photocatalytic reduction of Rh⁴⁺ species to Rh³⁺ by photo-excited electrons, as previously reported for SrTiO₃:Rh particles.^{16,28} No appreciable release of particles from the substrate was observed for WH-10' film after the reaction. On the other hand, the fraction of expose surface of substrate was appreciably increased in the SS-10' film after the reaction, indicating that a part of particles was detached from the substrate during the H₂ evolution reaction (see Fig. S6). Even the stirring the solution in dark resulted in particle release from the SS-10' film (not shown). These results indicated that the WH-films were mechanically more robust than the SS-films. The small particle sizes of WH-particles certainly allowed the sufficient contact among the particles in WH-film as well as the sufficient adhesion between particles and substrate.

Fig. 6 shows the dependence of film thickness on the H₂ evolution rates. The rates of H₂ evolution on the WH-films increased linearly with increasing thickness up to 5 μ m and gradually increased to reach maximum value at 10 μ m (3.2 μ mol/h). The rates of H₂ evolution on SS-films increased with increasing film thickness, however, saturated at a thinner thickness of 5 μ m. Up to 5 μ m, each WH-film showed nearly 4 times higher H₂ evolution rates than the corresponding SS-films with same thicknesses. As we recently reported, SrTiO₃:Rh particles prepared by the present WH-method showed higher photocatalytic activity for H₂ evolution than the SrTiO₃:Rh particles prepared by the SS-method. Indeed, the present WH-particles, which were prepared at 1000°C, showed ca. 4 times higher H₂ evolution rates than SS-particles prepared at the same temperature.²⁸ This finding strongly suggested that the higher photocatalytic activity of WH-particles dominantly contributed to the higher performance of WH-films for H₂ production. It

also should be noted that the H_2 evolution rates of WH-films increased as the film thickness increased up to 10 μm , while those of SS-films saturated as the film thickness at 5 μm . In the case of SS-film, large SS-particles ($> 300 \text{ nm}$) existing in the upper side certainly scattered back the incident photons partially, as well as absorbed, and consequently inhibited the light penetration into the bottom part, resulting in the saturated rate of H_2 evolution in the thicker films. In other word, a part of the particles in SS-films, especially those in bottom side, is unable to absorb the incident photons. On the other hand, in the case of WH-films, which consist of small WH-particles (ca. 50 nm), most of the particles effectively absorbed the light and functioned as photocatalyst due to the much less scattering of the incident light, consequently afforded the enhanced H_2 evolution with the increasing thickness up to 10 μm , while further increase in thickness resulted in the saturation because nearly all of the incident photons were absorbed within the films.

Influence of immobilization on the photocatalytic performance

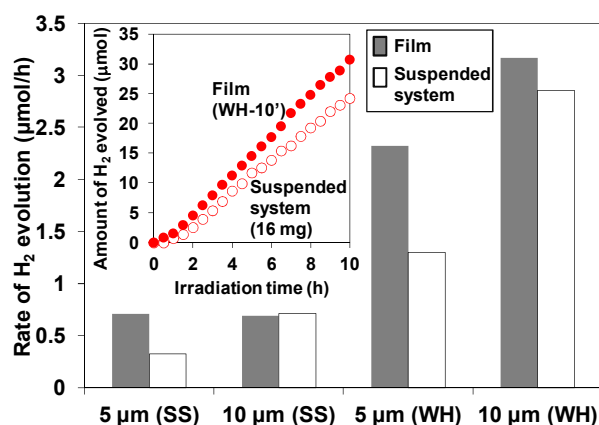
To evaluate the influence of immobilization on the performance, we compared the H_2 evolution rates on the films with those on the suspended particles. For example, the immobilization of the particles on substrates may lower diffusion of the substances (e.g., water) and/or the products (e.g., H_2 gas) inside the pores of film and therefore may decrease the H_2 evolution rate. The rates of H_2 evolution using suspended WH- or SS-particles or fixed WH- or SS- T ($T = 5, 10'$) films are summarized in Fig. 7. The amounts of particles loaded on each film with thickness of 5 and 10 μm were measured to be ca. 8 mg and 16 mg, respectively, regardless to the kind of particles (WH or SS). Thus, the same amounts of particles were used in suspended system for comparison. Except for SS-10', the films showed higher activity than the corresponding suspended systems employing the same amounts of photocatalyst particles. These results indicated that the $\text{SrTiO}_3\text{:Rh}$ particles immobilized on the films, especially in the case of WH-films, could absorb the light more efficiently than the suspended particles. The higher efficiency in the films were probably due to the more effective absorption of the photons by the neighboring particles in the densely packed film even if a part of incident photons was

Fig. 7 Rate of H_2 evolution from an aqueous methanol solution under visible light irradiation on a WH/SS- x film ($x = 5$ or $10'$) and from a $\text{SrTiO}_3\text{:Rh}$ -suspended system containing $\text{SrTiO}_3\text{:Rh}$ particles with the same amount as the film contains. Conditions: $3 \times 3 \text{ cm}$ film, 8 mg (5 μm) or 16 mg (10 μm) particles; reactant solution, 100 mL of 10 vol% aqueous methanol solution; light source, 300 W Xe lamp with cut-off filters ($\lambda > 410 \text{ nm}$).

scattered on the surface of particles. On the other hand, in the suspended systems, a portion of photons is scattered on the surface of particles and then uselessly passed through the diluted suspension, resulting in the lower efficiency than in the film systems. As for SS-10', the light can be used only on the upper side because of significant light scattering due to the large particle size, resulting in the similar rate of H_2 evolution to that on suspension system. The higher H_2 evolution rates in other films also implied that the diffusion of substances was not significantly lowered in the pores in the WH- and SS-films. However, the rates of gas evolution on the present $\text{SrTiO}_3\text{:Rh}$ films were still lower than those on general suspension systems for water splitting under visible light. The low evolution rates make it difficult to evaluate objectively the efficiency in the diffusion of substances and/or products in the present porous films. Thus, we prepared non-doped- SrTiO_3 porous films (10 μm) that are expected to evolve H_2 with much higher rates than the Rh-doped one, while the former required the irradiation of UV light. The non-doped- SrTiO_3 particles were prepared *via* same preparation procedure to that for Rh-doped- SrTiO_3 (WH-) particles, except for the absence of Rh-salt, producing the non-doped- SrTiO_3 having the same particles size (ca. 50 nm) to that of Rh-doped one. As shown in Fig. S7, the H_2 evolution rate on the SrTiO_3 porous film showed much higher rate (78 $\mu\text{mol/h}$) than that on Rh-doped one (3.2 $\mu\text{mol/h}$, under visible light). The H_2 evolution rate on the SrTiO_3 porous film was almost same with that on the corresponding suspended particles, strongly suggesting that the diffusion of substances and/or products was not significantly lowered in the pores in the present SrTiO_3 film systems, including Rh-doped one, prepared *via* screen-printing.

Effect of adding the light scattering centers on the photocatalytic performance

As shown above, the combination of the screen-printing method with $\text{SrTiO}_3\text{:Rh}$ particles prepared *via* the WH-method enable the fabrication of porous $\text{SrTiO}_3\text{:Rh}$ film that possess capability of evolving H_2 efficiently from aqueous methanol solution under visible light irradiation, in which the use of small WH-particle probably minimize the light scattering and enable the most of $\text{SrTiO}_3\text{:Rh}$ particles to absorb the incident light. However, too low scattering may result in the transmittance of a part of incident light without absorption in the WH-film. To solve the discrepancy between the light absorbance and scattering in the WH-film, we attempted to add small amounts of SS-particles, which have larger diameters and significantly scatter the light, into WH-particles that shows higher activity of H_2 evolution. For example, for the improvement of the photon-to-current efficiency in the dye-sensitized solar cell (DSSC), small amount of large TiO_2 particles ($> 200 \text{ nm}$) that scatter the visible light are often added into the nano-sized TiO_2 particles which absorb large amount of dye molecules and conduct electrons efficiently.²⁹⁻³³ Thus, we



expect that a part of incident visible light is scattered by the large SS-particles and subsequently absorbed by small WH-particles, resulting in more efficient utilization of incident light. We prepared films by screen-printing using the paste composed

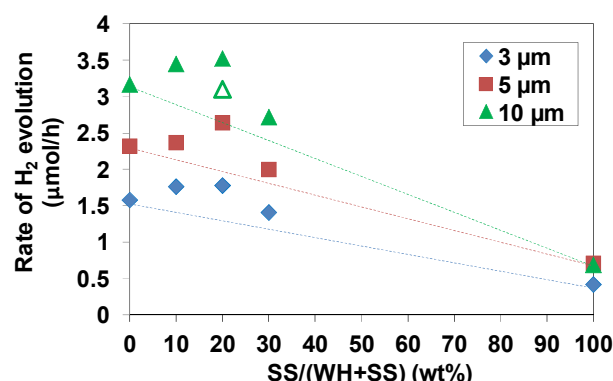


Fig. 8 Plots of the H_2 evolution rate from an aqueous methanol solution on films prepared with a mixture of WH- and SS-particles under visible light irradiation against the ratio of SS particles over the sum of WH- and SS-particles (weight%). Filled triangle, filled square, and filled diamond show films with 3, 5, and 10 μm -thickness. Open triangle shows a layered film consisted of WH-particles (80 wt%) over SS-film (20 wt%). The dashed lines indicate the expected rate based on the rates with pure WH- and SS-films. Conditions: 3×3 cm film; reactant solution, 100 mL of 10 vol% aqueous methanol solution; light source, 300 W Xe lamp with cut-off filters ($\lambda > 410$ nm).

of various ratios of WH- and SS-particles. The fractions of SS-particles X were 0, 10, 20, and 30 wt%. The resulting films are denoted as (WH+X-SS) hereafter. As shown in the SEM image of (WH+20-SS), for example, SS-particles were dispersed in the film homogeneously (see Fig. S8). Fig. 8 shows the relationship between the ratios of SS-particles added and the H_2 -evolution rate on the films with different thickness. The rate of H_2 evolution in every thickness increased with the increasing amounts of SS-particles up to 20 wt%, but decreased with further addition. If the WH- and SS-particles act independently as photocatalysts, the H_2 evolution rates should be simple sum of each contribution of WH- and SS-particles, as shown in Fig. 8 as dotted lines. However, the H_2 evolution rates on composite films were higher than the estimated values, also higher than those on pure WH-films. We also prepared the composite films (10 μm) in which SS-particles (10 wt%) exist only bottom side, for comparison. The H_2 evolution rate of this film was higher than that of the estimated value (see Fig 8, open triangle), but lower than the composite film in which the SS-particles dispersed homogeneously. These results strongly suggested that the composite films could use incident light more efficiently due to the light scattering by large SS-particles added into the films. The large SS-particles might also improved the diffusion of the substrates by forming larger pores in the film, as suggested in the previous report on photocatalyst panel of GaN-ZnO particles added by large SiO_2 particles (a few μm size).¹¹

Conclusion

In the present study, we attempt to fabricate the photocatalyst panels that can efficiently generate H_2 under visible light by employing highly active $\text{SrTiO}_3\text{:Rh}$ fine particles prepared *via* a water-based hetero-chelate method. The combination of the fine particles and screen-printing method enabled us to precisely

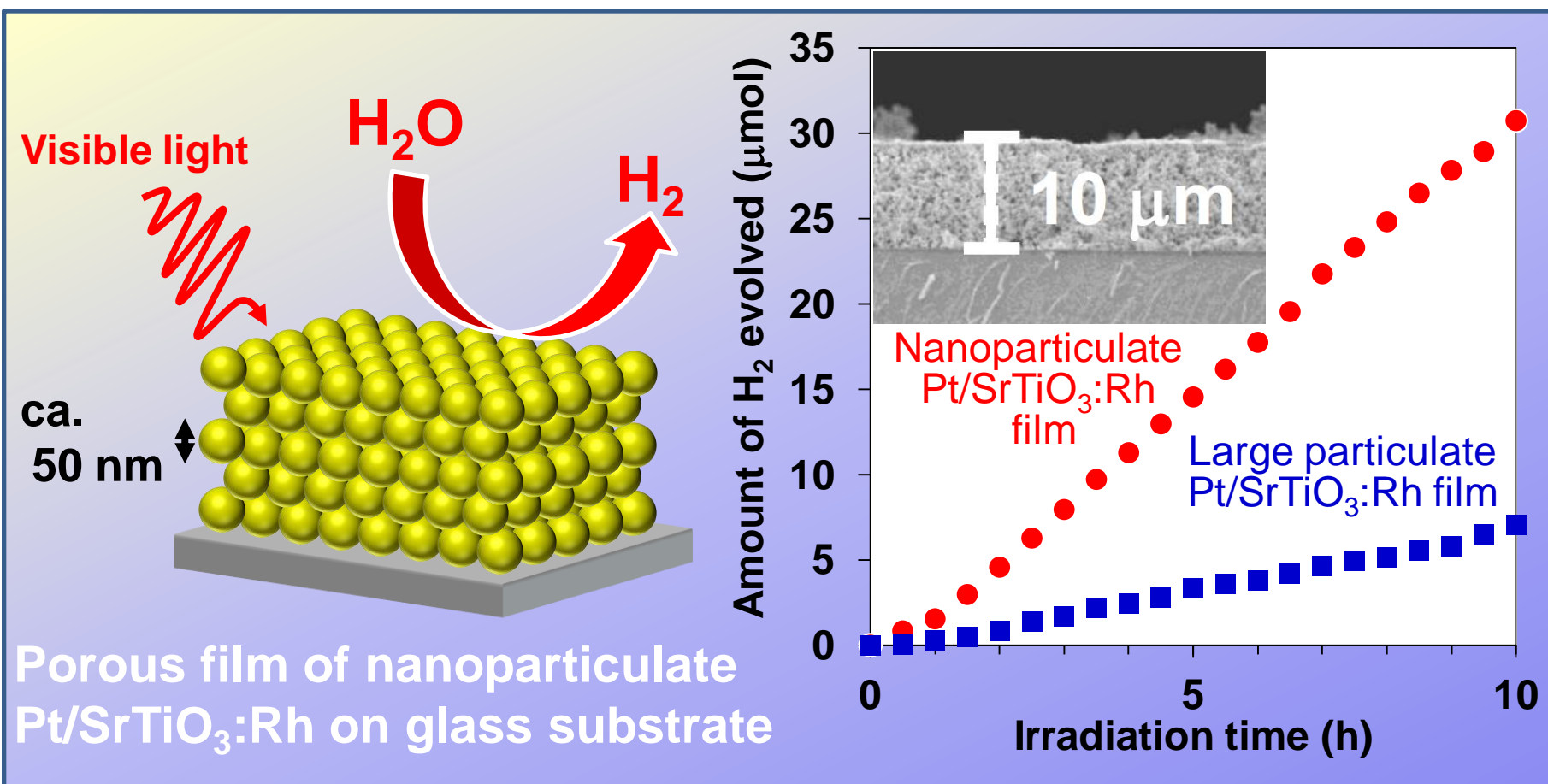
control the thickness (1 to 10 μm) of the porous films with enough mechanical strength after calcination (500°C) in air, whereas the use of large particle prepared *via* a conventional solid state reaction method resulted in inhomogeneous and uncontrollable thickness. The porous $\text{SrTiO}_3\text{:Rh}$ films prepared with fine particles exhibited almost linear increase in H_2 evolution rate with increasing film thickness up to 5 μm and gradually increased to reach maximum value at 10 μm ; the H_2 evolution rates on the films (5 and 10 μm) were higher than those on the suspended system using the same amounts of photocatalyst particles. These results indicate that the present photocatalyst panels, as assembled 2-D structure, can effectively utilize the incident light comparable to the conventional suspension systems. Efficient H_2 production on these panels also suggested that the transfer of substance and products was not significantly inhibited within the porous films. Moreover, the improvement of H_2 evolution rate by adding light scattering media (large $\text{SrTiO}_3\text{:Rh}$ particles) will provide an effective strategy for achieving highly efficient photocatalysis in fixed panels. Our concept of constructing highly active porous structure with fine photocatalyst particles *via* simple screen-printing method will provide the possibility of large-scale application of photocatalyst panels for practical splitting of water under solar light.

Notes and references

The authors have a patent application (International application number: WO2014203996A) on part of this work.

- 1 A. Fujishima and K. Honda, *Nature*, 1972, **238**, 37–38.
- 2 K. Maeda and K. Domen, *J. Phys. Chem. C*, 2007, **111**, 7851..
- 3 A. Kudo and Y. Miseki, *Chem. Soc. Rev.*, 2009, **38**, 253–278.
- 4 F. E. Osterloh, *Chem. Mater.* 2008, **20**, 35–54.
- 5 A. Kudo, *Mater. Res. Bull.*, 2011, **36**, 32–38.
- 6 R. Abe, *Bull. Chem. Soc. Jpn.*, 2011, **84**, 1000–1030.
- 7 K. Maeda, *ACS Catal.*, 2013, **3**, 1486–1503.
- 8 R. Abe, *J. Photochem. Photobiol. C. Photochem. C.*, 2010, **11**, 179–209.
- 9 T. Hisatomi, J. Kubota, K. Domen, *Chem.Soc. Rev.*, 2014, **43**, 7520.
- 10 F. E. Osterloh, *Chem.Soc. Rev.*, 2013, **42**, 2294.
- 11 A. Xiong, G. Ma, K. Maeda, T. Takata, T. Hisatomi, T. Setoyama, J. Kubota, K. Domen, *Catal Sci Tech.*, 2014, **4**, 325–328.
- 12 B.Pinaud, J. Benck, L.Seitz, A. Forman, Z. Chen, T. Deutsch, B. James, K. Baum, G. Baum, S. Ardo, H. Wang, E. Miller and T. Jaramillo, *Energy Environ. Sci.*, 2013, **6**, 1983
- 13 Q. Wang, Y. Li, T. Hisatomi, M. Nakabayashi, N. Shibata, J. Kubota, K. Domen, *J. Catal.*, 2015, **328**, 308–315.
- 14 K. Takanabe, K. Domen, *Chem Cat Chem*, 2012, **4**, 1485.
- 15 C. Agrafiotis, A. Tsetsekou, *J. Eur. Ceram. Soc.*, 2000, **20**, 815–824.
- 16 R. Konta, T. Ishii, H. Kato and A. Kudo, *J. Phys. Chem. B*, 2004, **108**, 8992–8995.
- 17 H. Kato, M. Hori, R. Konta, Y. Shimodaira and A. Kudo, *Chem. Lett.*, 2004, **33**, 1348–1349.
- 18 H. Kato, Y. Sasaki, A. Iwase and A. Kudo, *Bull. Chem. Soc. Jpn.*, 2007, **80**, 2457–2464.

- 19 Y. Sasaki, A. Iwase, H. Kato and A. Kudo, *J. Catal.*, 2008, **259**, 133-137.
- 20 Y. Sasaki, H. Nemoto, K. Saito and A. Kudo, *J. Phys. Chem. C*, 2009, **113**, 17536–17542.
- 21 A. Iwase, Y. H. Ng, Y. Ishiguro, A. Kudo and R. Amal, *J. Am. Chem. Soc.*, 2011, **133**, 11054–11057.
- 22 H. Kato, Y. Sasaki, N. Shirakura and A. Kudo, *J. Mater. Chem. A*, 2013, **1**, 12327–12333.
- 23 Y. Sasaki, H. Kato and A. Kudo, *J. Am. Chem. Soc.*, 2013, **135**, 5441.
- 24 S. S. K. Ma, K. Maeda, T. Hisatomi, M. Tabata, A. Kudo and K. Domen, *Chem.–Eur. J.*, 2013, **19**, 7480–7486.
- 25 Q. Jia, A. Iwase, A. Kudo, *Chem. Sci.*, 2014, **5**, 1513-1519
- 26 Q. Wang, T. Hisatomi, S. S. K. Ma, Y. Li, K. Domen, *Chem. Mater.*, 2014, **26**, 4144–4150.
- 27 S. Okunaka, H. Tokudome, Y. Hitomi and R. Abe, *J. Mater. Chem. A*, 2015, **3**, 1688–1695.
- 28 S. Okunaka, H. Tokudome and R. Abe, *J. Mater. Chem. A*, 2015, in press DOI: 10.1039/C5TA02903A
- 29 C. J. Barbè, F. Arendse, P. Comte, M. Jirousek, F. Lenzmann, V. Shkolover, M. Grätzel, *J. Am. Ceram. Soc.* 1997, **80** (12), 3157-3171.
- 30 T. G. Deepak, G. S. Anjusree, S. Thomas, T. A. Arun, S. V. Nair and A. S. Nair, *RSC Adv.*, 2014, **4**, 17615-17638.
- 31 A. Usami, *Chem. Phys. Lett.*, 1997, **277**, 105.
- 32 S. Hore, C. Vatter, R. Kern, H. Smit and A. Hinsch, *Sol. Energy mater. Sol. Cells*, 2006, **90**, 1176.
- 33 J.-K. Lee, B.-H. Jeong, S. J. Y.-G. Kim, Y.-W. Jang, S.-B. Lee and M.-R. Lim, *J. Ind. Eng. Chem.*, 2009, **15**, 724.



Photocatalytic H₂ evolution is demonstrated under visible light on porous films of Rh-doped SrTiO₃ nanoparticles.